nature medicine

Rescue of hearing and vestibular function by antisense oligonucleotides in a mouse model of human deafness

Jennifer J Lentz[1,6], Francine M Jodelka[2,6], Anthony J Hinrich[2,6], Kate E McCaffrey[2], Hamilton E Farris[1], Matthew J Spalitta[1], Nicolas G Bazan[3], Dominik M Duelli[4], Frank Rigo[5] & Michelle L Hastings[2]

Hearing impairment is the most common sensory disorder, with congenital hearing impairment present in approximately 1 in 1,000 newborns[1]. Hereditary deafness is often mediated by the improper development or degeneration of cochlear hair cells[2]. Until now, it was not known whether such congenital failures could be mitigated by therapeutic intervention[3–5]. Here we show that hearing and vestibular function can be rescued in a mouse model of human hereditary deafness. An antisense oligonucleotide (ASO) was used to correct defective pre-mRNA splicing of transcripts from the *USH1C* gene with the c.216G>A mutation, which causes human Usher syndrome, the leading genetic cause of combined deafness and blindness[6,7]. Treatment of neonatal mice with a single systemic dose of ASO partially corrects *Ush1c* c.216G>A splicing, increases protein expression, improves stereocilia organization in the cochlea, and rescues cochlear hair cells, vestibular function and low-frequency hearing in mice. These effects were sustained for several months, providing evidence that congenital deafness can be effectively overcome by treatment early in development to correct gene expression and demonstrating the therapeutic potential of ASOs in the treatment of deafness.

Usher syndrome is characterized by hearing impairment combined with retinitis pigmentosa and, in some cases, vestibular dysfunction. The frequency in the general population may be as high as 1 in 6,000 (ref. 8). Type 1 Usher syndrome is characterized by profound hearing impairment and vestibular dysfunction at birth and the development of retinitis pigmentosa in early adolescence. Approximately 6–8% of type 1 Usher syndrome cases are caused by mutations in the *USH1C* gene[9], which encodes the protein harmonin. The *USH1C*216G>A (216A) mutation accounts for all cases of type 1 Usher syndrome in Acadian populations[9–11] and creates a cryptic 5′ splice site that is used preferentially over the authentic 5′ splice site of exon 3 (**Fig. 1a**), resulting in a frameshift and truncated harmonin protein[12].

We used a mouse model of Usher syndrome based on the human 216A mutation[13] to investigate a treatment for deafness and vestibular dysfunction using ASOs (**Supplementary Fig. 1**) designed to redirect cryptic splicing of 216A pre-mRNA to the authentic site (**Fig. 1a**). To screen for ASOs that block 216A cryptic splicing, we transfected a minigene expression plasmid composed of exons 2–4 and the intervening introns of human *USH1C* (wild type) or *USH1C* 216A into HeLa cells with 47 different individual ASOs surrounding the mutation and quantified splicing correction (**Fig. 1b** and **Supplementary Table 1**). Several ASOs blocked cryptic splicing and promoted correct splicing (**Fig. 1b**,**c**) in a dose-dependent manner (**Fig. 1d**). The ASOs also blocked cryptic splicing, promoted correct splicing of the endogenous *Ush1c* 216A gene transcript and increased harmonin protein expression in a mouse kidney cell line derived from mice homozygous for the *Ush1c* 216A mutation (216AA mice) (**Supplementary Fig. 2**). ASOs induced correct splicing *in vivo* after a series of intraperitoneal injections of 50 mg per kg body weight of ASO in adult 216AA mice (**Fig. 1e**). ASO-29 promoted the highest amount of correct splicing of the ASOs tested (**Fig. 1e**) and also corrected splicing and increased harmonin protein expression (**Fig. 1f**,**g** and **Supplementary Fig. 3**) in a dose-dependent manner.

216AA mice are deaf and have severe vestibular dysfunction, as indicated by their auditory brainstem response (ABR) and head-tossing and circling behavior[13,14]. Neonatal 216AA mice were injected intraperitoneally with 300 mg per kg body weight of ASO-C or ASO-29 to test whether ASO-29 can correct vestibular and hearing defects. 216AA mice untreated or treated with a mismatched ASO (ASO-C) showed circling behavior, whereas 216AA mice treated with ASO-29 did not circle, and showed similar behavior to heterozygous (216GA) or wild-type (216GG) mice (**Fig. 2a**,**b** and **Supplementary Video 1**). We did not observe any circling behavior in mice treated with ASO-29 at postembryonic day 3 (P3), P5, P10 or P13, whereas 216AA mice treated on P16 showed circling behavior similar to untreated or ASO-C–treated 216AA mice (**Fig. 2b**). ASO-29–treated 216AA mice had no vestibular dysfunction at 6 months of age (**Supplementary Fig. 4a**). We performed trunk-curl, contact-righting and swim tests on 2- to 3-month-old and 6- to 9-month-old mice to further quantify vestibular function[15]. The younger and older 216AA mice all performed poorly in these tests, whereas 216AA mice treated with ASO-29 at P5 performed similarly to untreated or ASO-C–treated 216GA mice and showed no vestibular dysfunction (**Supplementary Fig. 4b**). Our

[1]Neuroscience Center and Department of Otorhinolaryngology & Biocommunications, Louisiana State University Health Sciences Center (LSUHSC), New Orleans, Louisiana, USA. [2]Department of Cell Biology and Anatomy, Chicago Medical School, Rosalind Franklin University of Medicine and Science, North Chicago, Illinois, USA. [3]Neuroscience Center and Department of Ophthalmology, LSUHSC, New Orleans, Louisiana, USA. [4]Department of Cellular and Molecular Pharmacology, Chicago Medical School, Rosalind Franklin University of Medicine and Science, North Chicago, Illinois, USA. [5]Isis Pharmaceuticals, Carlsbad, California, USA. [6]These authors contributed equally to this work. Correspondence should be addressed to M.L.H. (michelle.hastings@rosalindfranklin.edu) or J.J.L. (jlentz@lsuhsc.edu).

Received 12 September 2012; accepted 28 January 2013; published online 4 February 2013; doi:10.1038/nm.3106

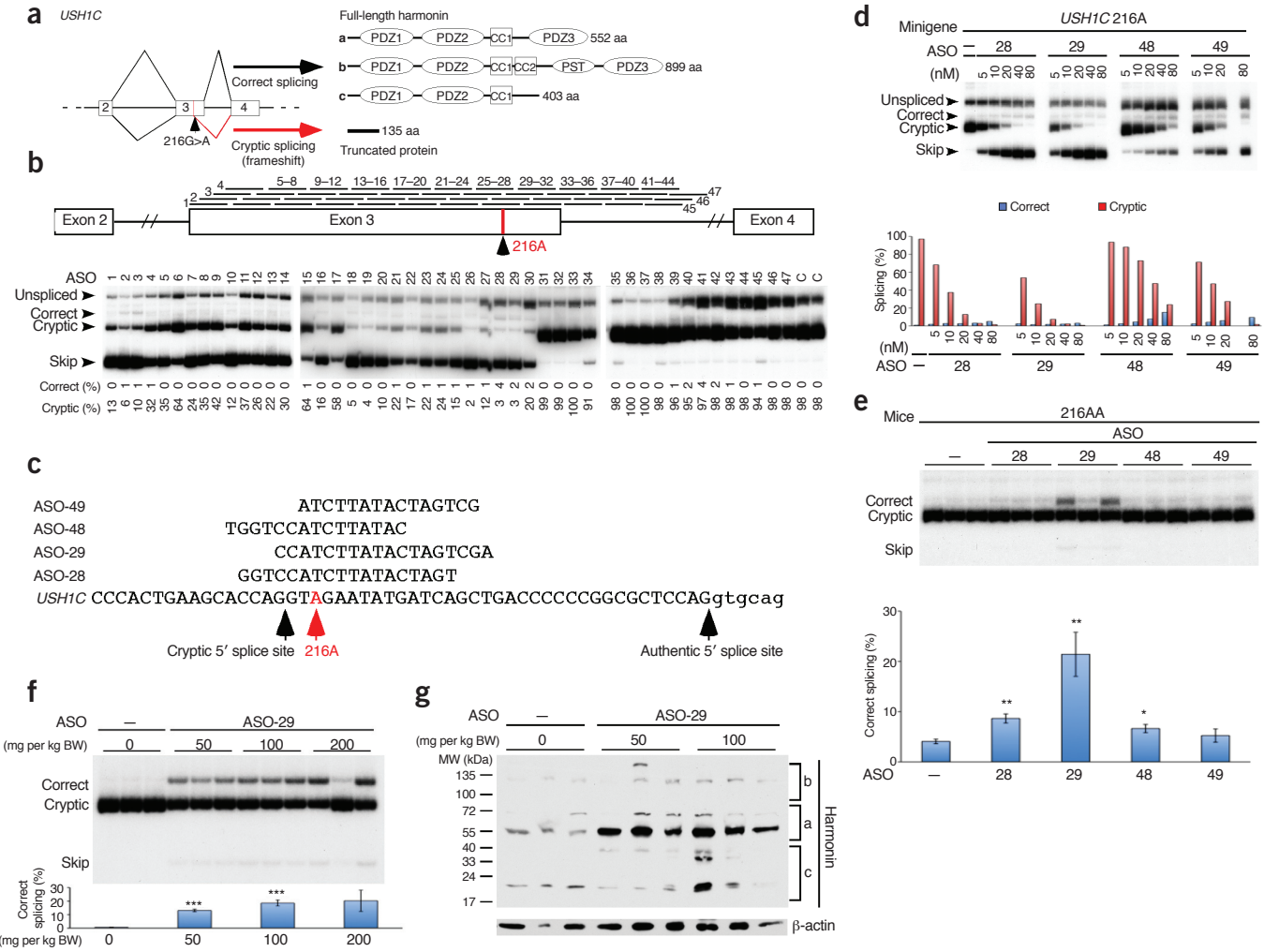

Figure 1 Correction of *USH1C* 216A splicing using ASOs. (**a**) Gene structure of *USH1C* exons 2–4 and RNA splicing and protein products. Boxes represent exons and lines are introns. Diagonal lines indicate splicing. The locations of the 216A mutation and the cryptic splice site are labeled. aa, amino acids; PDZ, PSD95-Dlg1-zo1-domain; CC, coiled-coil domain; PST, proline-serine-threonine–rich domain. (**b**) Top, diagram of ASOs tested below, mapped to their position of complementarity on *USH1C*. Bottom, radioactive RT-PCR of RNA isolated from HeLa cells transfected with a *USH1C* 216A minigene and the indicated ASO at a final concentration of 50 nM. RNA spliced forms are labeled. 'Unspliced' refers to transcripts with intron 3 retained, and 'skip' indicates exon 3 skipping. (Below) Quantification of the percentage splicing in graph is calculated as: Correct (%) = [(correct/(correct + cryptic + skip)] × 100, and Cryptic (%) = [(cryptic/(correct + cryptic + skip)] × 100. 'C' indicates mock-treated control. (**c**) Sequence and *USH1C* target region of ASOs. Exonic and intronic sequences are in capital and lower-case letters, respectively. (**d**) Analysis of *USH1C* 216A minigene transcript splicing in HeLa cells treated with increasing concentrations of the indicated ASOs from **c**. Quantification of percentage correct and percentage cryptic splicing is shown in graph (below). (**e**) RT-PCR analysis of RNA isolated from kidneys of adult 216AA mice 24 h after final injection of 50 mg per kg body weight (BW) of different ASOs. Samples from three individual mice are shown. *Ush1c* spliced products are indicated and quantified in graph (below) as described above. Error bars represent s.e.m. (*$P \leq 0.05$, **$P \leq 0.01$, $n = 3$, two-tailed Student's *t*-test compared to vehicle treatment). (**f**) RT-PCR analysis of RNA isolated from kidneys of adult *Ush1c* 216AA mice treated with different doses of ASO-29. Samples from three individual mice are shown. *Ush1c* spliced products are indicated and quantified as described above. Error bars represent s.e.m. (***$P \leq 0.001$, $n = 3$, two-tailed Student's *t*-test compared to vehicle). (**g**) Immunoblot analysis of harmonin protein in lysates from the kidneys of adult 216AA mice analyzed in **f**. Blots were also probed with a β-actin–specific antibody for a loading reference. MW, molecular weight.

results suggest that ASOs can prevent vestibular dysfunction associated with Usher syndrome in mice when delivered neonatally.

Treatment of 216AA mice with ASO-29 also rescued hearing. Startle responses to high-amplitude sound are similar in ASO-29–treated 216AA and either ASO-C–treated or untreated 216GA mice (**Supplementary Video 2** and **Supplementary Fig. 5**). 216AA mice treated with ASO-C, however, showed neither an initial startle response, defined as an ear twitch and rapid head and body movement, nor a subsequent freezing response after acoustic stimulus (**Supplementary Video 2**). We recorded auditory-evoked brainstem responses to quantitatively assess hearing function. We recorded responses to different sound frequencies (8–32 kHz and broad band noise, BBN) at different intensities (18–90 dB SPL). Hearing thresholds represent the lowest sound intensity at which a recognizable ABR wave (neural response) is observed. We compared ABR thresholds in P30 216AA mice treated with ASO-29, treated and untreated 216GG wild-type and 216GA heterozygous mice, and 216AA mutant mice treated with ASO-C. 216GG and 216GA mice had thresholds typical of mice with normal hearing (**Fig. 2c**,**d**). Similar to untreated 216AA mice[14], 216AA mice treated with ASO-C had abnormal or absent ABRs (**Fig. 2c**,**d** and **Supplementary Fig. 6**). 216AA mice treated between P3 and P5 with a single dose of ASO-29

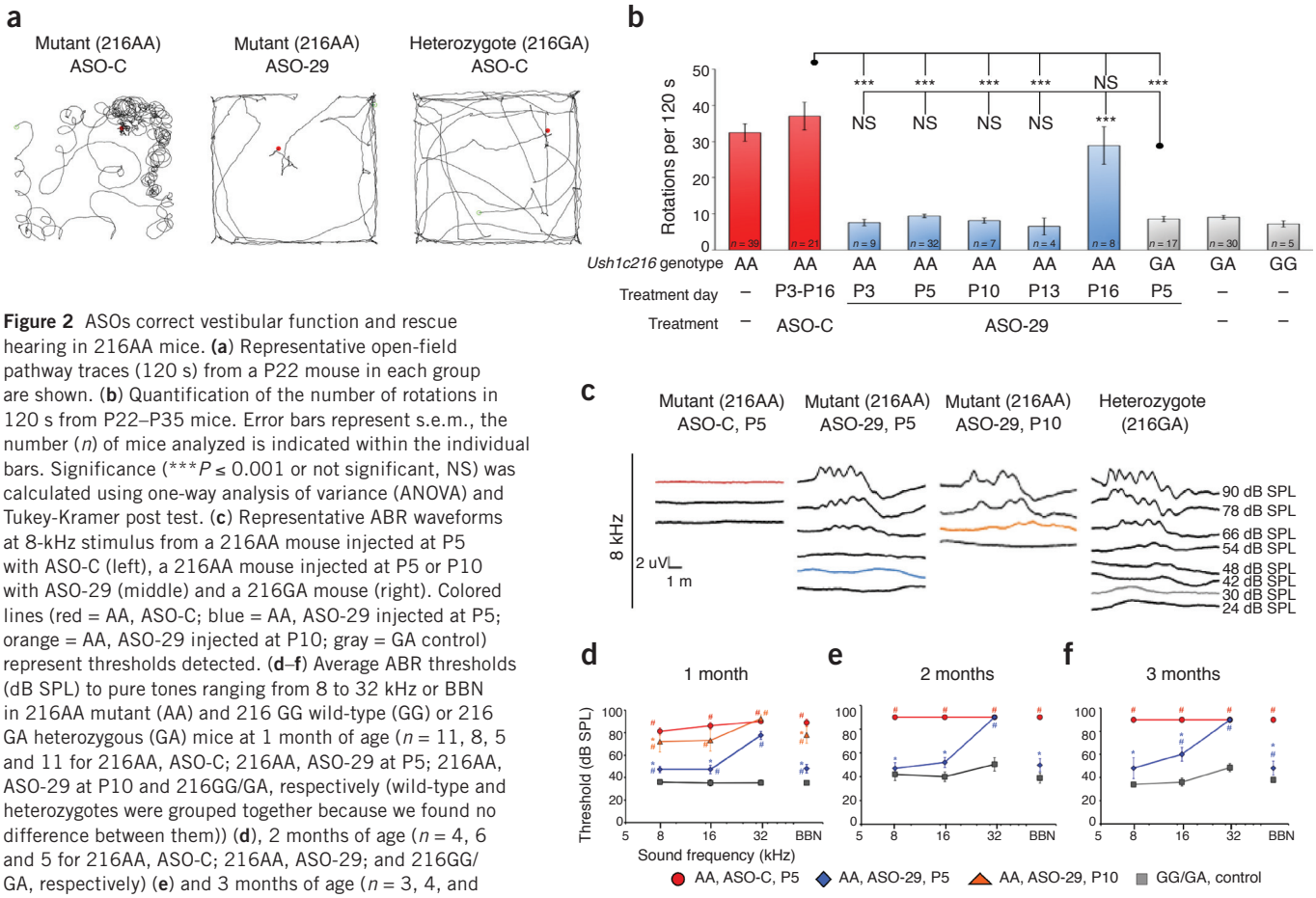

Figure 2 ASOs correct vestibular function and rescue hearing in 216AA mice. (**a**) Representative open-field pathway traces (120 s) from a P22 mouse in each group are shown. (**b**) Quantification of the number of rotations in 120 s from P22–P35 mice. Error bars represent s.e.m., the number (*n*) of mice analyzed is indicated within the individual bars. Significance (***$P \leq 0.001$ or not significant, NS) was calculated using one-way analysis of variance (ANOVA) and Tukey-Kramer post test. (**c**) Representative ABR waveforms at 8-kHz stimulus from a 216AA mouse injected at P5 with ASO-C (left), a 216AA mouse injected at P5 or P10 with ASO-29 (middle) and a 216GA mouse (right). Colored lines (red = AA, ASO-C; blue = AA, ASO-29 injected at P5; orange = AA, ASO-29 injected at P10; gray = GA control) represent thresholds detected. (**d**–**f**) Average ABR thresholds (dB SPL) to pure tones ranging from 8 to 32 kHz or BBN in 216AA mutant (AA) and 216 GG wild-type (GG) or 216 GA heterozygous (GA) mice at 1 month of age ($n = 11$, 8, 5 and 11 for 216AA, ASO-C; 216AA, ASO-29 at P5; 216AA, ASO-29 at P10 and 216GG/GA, respectively (wild-type and heterozygotes were grouped together because we found no difference between them)) (**d**), 2 months of age ($n = 4$, 6 and 5 for 216AA, ASO-C; 216AA, ASO-29; and 216GG/GA, respectively) (**e**) and 3 months of age ($n = 3$, 4, and 4 for 216AA, ASO-C; 216AA, ASO-29; and 216GG or GA, respectively) (**f**). Error bars represent s.e.m. * indicates a significant difference between ASO-29–treated 216AA and ASO-C–treated 216AA mice, and # indicates a significant difference between ASO-29–treated 216AA and 216GA control mice ($P \leq 0.05$; two-way ANOVA with Tukey-Kramer post test).

had recognizable waveforms and near-normal thresholds to BBN and 8- and 16-kHz pure tones when compared to 216GG and 216GA control mice (**Fig. 2c**,**d** and **Supplementary Fig. 6**). The thresholds of ASO-29–treated 216AA mice at 32 kHz were not significantly different than those of control ASO-C–treated 216AA mice, indicating that treatment was not effective at rescuing high-frequency hearing (**Fig. 2d**). These data show rescue of low- and mid-frequency hearing at P30 in ASO-29–treated 216AA mice. 216AA mice treated with ASO-29 at P10 had significantly higher thresholds than those treated at P3–P5 but significantly lower thresholds in response to BBN and an 8-kHz tone than untreated mutants or mutants treated with ASO-C ($P \leq 0.05$) (**Fig. 2c**,**d** and **Supplementary Fig. 6**), implying a developmental window of therapeutic efficacy in mice. At 2 months of age, 216AA mice treated at P3–P5 had ABR thresholds to BBN and 8 kHz and 16 kHz, but not 32 kHz, equivalent to 216GG and 216GA mice ($P \leq 0.05$, **Fig. 2e** and **Supplementary Fig. 7a**–**d**). At 3 months, there was no significant difference in ABR thresholds at 8 kHz between control 216GA heterozygous mice and 216AA mutant mice treated with ASO-29 at P3–P5 ($P \leq 0.05$), but the data show some loss of sensitivity in ASO-29–treated 216AA mice to 16 kHz and BBN (**Fig. 2f** and **Supplementary Fig. 8a**–**d**). At 6 months of age, there were significant differences in ABR thresholds between control 216GA or ASO-C–treated 216GG mice and ASO-29–treated 216AA mice at all frequencies ($P \leq 0.05$), though ASO-29–treated 216AA mice showed ABR thresholds that were significantly lower than those of ASO-C–treated 216AA mice ($P \leq 0.05$) (**Supplementary Fig. 9a**,**b**). These results suggest that mice injected with a single ASO treatment early in life can hear at 6 months of age, indicating a long-term, if slowly declining, therapeutic rescue of hearing.

To determine the effect of ASOs on *Ush1c* mRNA splicing and harmonin expression, we analyzed the cochleae from mice injected at P5 with ASO-29 or ASO-C. At P30, we observed a low amount of correct exon 3 splicing in the ASO-29–treated 216AA mice (**Fig. 3a**). Correct splicing peaked at P120, and expression of the full-length mRNA transcript at P180 was similar to that at P30, indicating that the effect of the ASO on splicing is stable and corresponds with ABR results at this time point (**Supplementary Fig. 9c**). Harmonin protein abundance was also higher in cochleae from ASO-29–treated 216AA mice compared to 216AA mice treated with ASO-C and similar to harmonin levels at P32–P35 in the cochleae of control 216GA mice (**Fig. 3b** and **Supplementary Fig. 10**).

The harmonin b isoform (**Fig. 1a**) localizes to the developing and mature stereocilia bundle of cochlear hair cells[16–19], where it is hypothesized to scaffold the molecular components of the mechanotransduction machinery[20]. We examined the expression and localization of harmonin b in microdissected organs of Corti from P30 216AA mice injected at P5 with either ASO-29 or ASO-C and untreated 216GA heterozygous littermates. Harmonin b was abundantly expressed in the tips of outer hair cell stereocilia bundles of 216GA mice, whereas the 216AA mice had less expression and it was mislocalized in the atypical bundles (**Fig. 3c**,**d**).

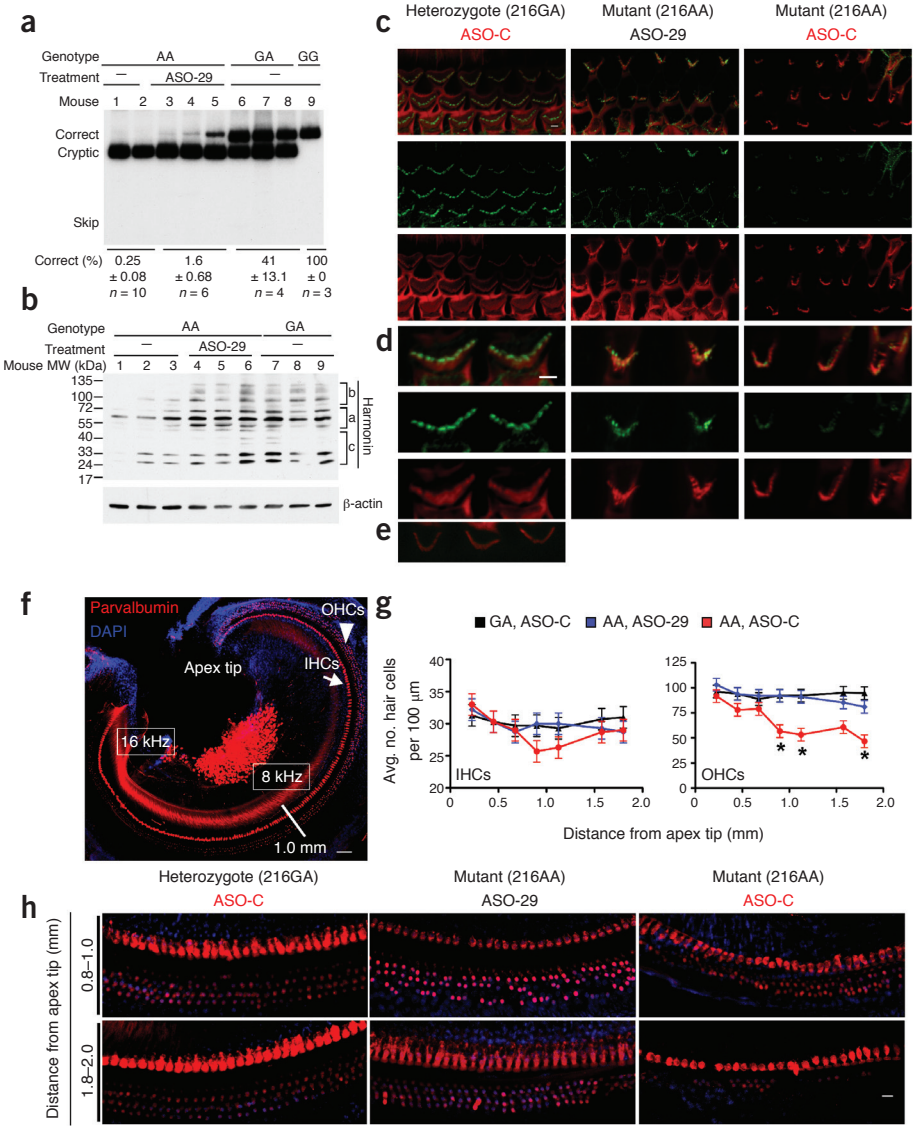

Figure 3 ASO-29 treatment corrects mRNA splicing and harmonin protein expression and prevents cochlear hair cell loss in 216AA mice. (**a**) RT-PCR analysis of cochlear RNA isolated at P32–P35 from mice treated with control (ASO-C) or ASO-29 at P3–P5. Spliced products are labeled. (**b**) Immunoblot analysis of harmonin expression in cochlea isolated at P32–35 from mice that were treated at P5. Different isoforms of harmonin expressed from *Ush1c* are labeled. Blots were also probed with a β-actin–specific antibody for a loading reference. (**c**) Immunofluorescence staining of harmonin b (green) and F-actin (red, phalloidin) in outer hair cell (OHC) bundles in the region of the basilar membrane that corresponds to hearing at 8 kHz (0.8–1.5 mm from apex tip). Images are from 216GA mice (left), 216AA mice treated with ASO-29 at P5 (middle) or 216AA mice treated with ASO-C at P5 (right). Scale bar, 3 μm. (**d**) Digital magnification (2× zoom) of images shown in **c**. Scale bar, 2 μm. (**e**) Immunofluorescence image of a primary antibody isotype control from a 216GA mouse taken from a similar OHC bundle location. (**f**) Immunofluorescence image of the regions of the basilar membrane that are represented in **g** and **h**. Hair cells are labeled with parvalbumin (red), and nuclei are counterstained with DAPI (blue). Scale bar, 50 μm. IHCs, inner hair cells. (**g**) Cochleogram showing inner (left) and outer (right) hair cell counts from regions progressively distant from the apex tip. Error bars represent the s.e.m. (*$P \leq 0.05$; $n = 3$ mice). At least 100 cells from each experimental group were evaluated for each region. (**h**) Immunofluorescence images of representative regions along the basilar membrane 0.8–1.0 mm (top) or 1.8–2.0 mm (bottom) from the extreme apex from P35 216GA mice treated with ASO-C at P5 (left), 216AA mice treated with ASO-29 at P5 (middle) or 216AA mice treated with ASO-C at P5 (right). Scale bar, 20 μm.

ASO-29–treated 216AA mice had elevated harmonin b expression with localization at the tips of stereocilia similar to that in the 216GA mice (**Fig. 3c**,**d**). These results suggest proper localization of harmonin with ASO treatment.

Frequency place-mapping in the mouse cochlea[21,22] suggests that the region corresponding to 8–16 kHz (the frequencies most robustly rescued by ASO-29) is located approximately 1–2 mm from the apex tip (**Fig. 3f**). To assess the relationship between hair cell number and ABR threshold, we counted hair cells labeled with parvalbumin. At P35, 216AA mice had significant outer hair cell loss from approximately 0.8–2.0 mm from the apex, corresponding to hearing at 6–20 kHz ($P \leq 0.05$) (**Fig. 3g**,**h**). In contrast, the number of outer hair cells in this region of 216AA mice treated with ASO-29 at P3–P5 did not differ from that in 216GA mice, which is consistent with rescued physiological function (**Fig. 3g**,**h**).

We also assessed changes in hair cell morphology that may reflect the rescue of hearing in the regions of the cochlea sensitive to 8 and 16 kHz. By P35, 216AA mice had significant hair cell loss in this region (**Fig. 3**); therefore, we analyzed subcellular structures in P18 216AA and 216GA mice before the loss of hair cells. We quantified the number of stereocilia bundles with typical 'U' or 'W' bundle shapes (**Fig. 4a**,**b**). The 216AA mice treated with ASO-29 had significantly fewer atypical bundles in the regions that detect 8 (0.8–1.2 mm) and 16 kHz (1.8–2.2 mm) ($P \leq 0.05$) but not in the region detecting 32 kHz (3.8–4.2 mm) (**Fig. 4c**). This pattern of anatomical stereocilia rescue is consistent with the ABR results showing a rescue of hearing in the 8- and 16-kHz range and less robust rescue in the 32-kHz range. Together, our results indicate a change in the bundle structure and number of hair cells at the apical–mid regions in ASO-29–treated 216AA mice, providing an anatomical correlate to function.

Our study demonstrates that a human disease–causing mutation can be corrected to treat deafness and vestibular dysfunction in a mouse model. Treatment during the critical hair cell developmental period is probably necessary and perhaps sufficient for long-term rescue of hearing. Notably, a modest correction of *Ush1c* mRNA splicing and expression of full-length harmonin is sufficient to rescue hearing in mice for 6 months. This enduring effect of the ASOs is consistent with the duration of action of ASOs observed in other mouse models of disease such as spinal muscular atrophy[23] and myotonic dystrophy[24].

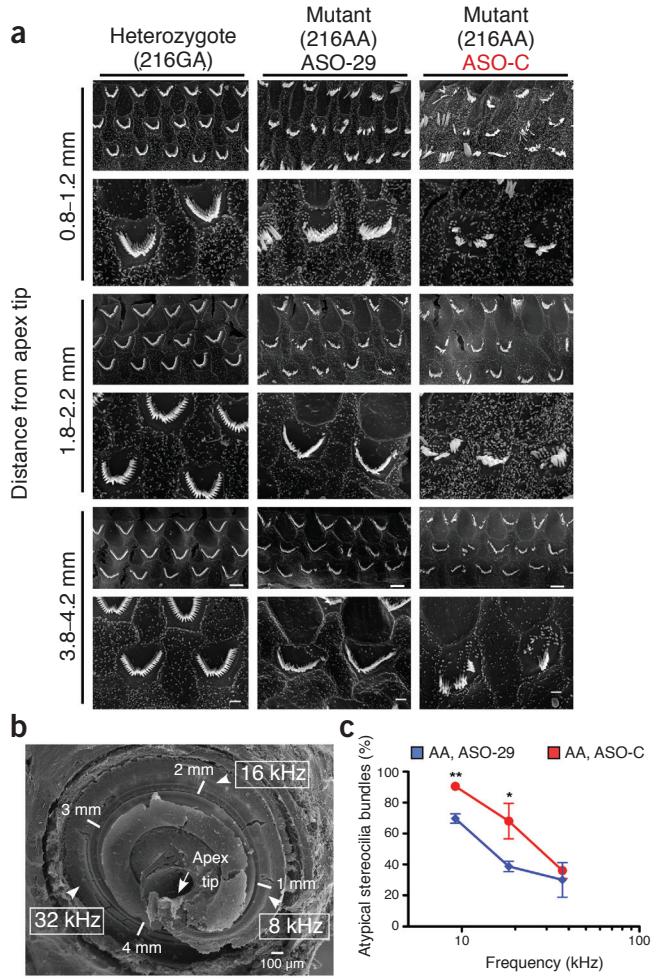

Figure 4 Restoration of hair cell stereocilia bundle shape in mice. (**a**) Scanning electron micrographs of outer hair cell bundles from P18 216GA and 216AA mice treated at P5 with ASO-C or ASO-29. Distance (mm) was measured from apex tip. Scale bars represent 1 μm and 10 μm for the high- and low-magnification images, respectively. (**b**) Scanning electron micrograph illustrating the regions of the cochlea that are represented in **a**. Scale bar, 100 μm. (**c**) Quantification of atypical bundles shown as a percentage of total cells counted at different positions along the basilar membrane in 216AA mice treated either with ASO-29 (blue line) or ASO-C (red line) (*$P \leq 0.05$, **$P \leq 0.005$; two-tailed unpaired *t*-test; $n = 3$ or 4 mice per region). Error bars represent s.e.m. At least 200 cells from each experimental group were evaluated with at least 60 hair cells from each region. 216GA control mice have no atypical bundles (data not shown).

The rescue of hearing in mice by ASO-29 treatment demonstrates that deafness can be treated if intervention occurs early in development. Treatment at P10 corrects vestibular function and partially restores hearing, whereas treatment at P3–P5 rescues vestibular function and hearing with ABRs comparable to those of wild-type mice (**Supplementary Fig. 1**). Although *Ush1c* is expressed as early as embryonic day 15 in mice[25,26], there is a peak of developmental expression in the cochlea that occurs after P4 and before P16 (https://shield.hms.harvard.edu/viewgene.html?gene=Ush1c). Our results are consistent with this expression pattern, suggesting that high expression before P5 is not required for the development of low- and mid-frequency hearing, but expression between P5 and P10 may be crucial. Hearing at high frequencies (32 kHz) is not rescued to the same level as that at the lower frequencies, and the rescue is more transient (**Fig. 2**). Because detection of high-frequency sound occurs at the base of the cochlea, this result may suggest that *Ush1c* is expressed tonotopically during development and that splicing correction at P5 benefits only the 30. apical-mid regions of the cochlea. The development of the ear and hearing in humans occurs *in utero*[27]. Thus, treatment in humans would probably require delivery to the fetus via approaches such as intrauterine transfusion[28].

Individuals with Usher syndrome present with both hearing and vision loss, and the correction of one of these sensory deficits may have a considerable positive impact. Although the retinitis pigmentosa associated with Usher syndrome is recapitulated in the 216AA mice, their retinal cell loss occurs later, at approximately 1 year of life[14]. Thus, our analysis of vision in these mice will require further investigation at later time points. The rescue of hearing in this study offers a model for studying the development of hearing and vestibular function and for developing approaches to correct these processes when they are impaired.

METHODS

Methods and any associated references are available in the online version of the paper.

Note: Supplementary information is available in the online version of the paper.

ACKNOWLEDGMENTS

We gratefully acknowledge support from the Hearing Health Foundation, Midwest Eye-Banks, the National Organization for Hearing Research Foundation, Capita Foundation and the US National Institutes of Health. We thank D. Cunningham and E. Rubel for assistance with scanning electron microscopy analysis; A. Rosenkranz, R. Marr and M. Oblinger for use of equipment; J. Huang for assistance with open-field analysis, L. Ochoa for assistance with ABR analysis computer support, G. MacDonald for assistance with confocal imaging and deconvolution analysis, U. Wolfrum (Johannes Gutenberg University of Mainz) for harmonin b–specific antibodies, H. Thompson for statistical analysis, and A. Case, B. Keats and M. Havens for discussions and comments on the manuscript.

AUTHOR CONTRIBUTIONS

The project was conceived of by M.L.H. Experiments were designed and performed by A.J.H., F.M.J., J.J.L., K.E.M., M.L.H. and D.M.D., and were analyzed by M.L.H., J.J.L., F.R., F.M.J., A.J.H. and K.E.M. Animal work was carried out by M.L.H., D.M.D., K.E.M., A.J.H., F.M.J., J.J.L. and M.J.S. Molecular experiments were performed by A.J.H., F.M.J., K.E.M. and M.L.H. J.J.L. carried out the immunofluorescence analysis. J.J.L., M.J.S. and H.E.F. performed auditory brainstem response experiments, and J.J.L. and N.G.B. interpreted the results. M.L.H. and J.J.L. wrote the paper.

COMPETING FINANCIAL INTERESTS

The authors declare competing financial interests: details are available in the online version of the paper.

1. Morton, C.C. & Nance, W.E. Newborn hearing screening—a silent revolution. *N. Engl. J. Med.* **354**, 2151–2164 (2006).
2. Dror, A.A. & Avraham, K.B. Hearing loss: mechanisms revealed by genetics and cell biology. *Annu. Rev. Genet.* **43**, 411–437 (2009).
3. Conde de Felipe, M.M., Feijoo Redondo, A.F., Garcia-Sancho, J., Schimmang, T. & Alonso, M.B. Cell- and gene-therapy approaches to inner ear repair. *Histol. Histopathol.* **26**, 923–940 (2011).
4. Di Domenico, M. *et al.* Towards gene therapy for deafness. *J. Cell. Physiol.* **226**, 2494–2499 (2011).
5. Bermingham-McDonogh, O. & Reh, T.A. Regulated reprogramming in the regeneration of sensory receptor cells. *Neuron* **71**, 389–405 (2011).
6. Bitner-Glindzicz, M. *et al.* A recessive contiguous gene deletion causing infantile hyperinsulinism, enteropathy and deafness identifies the Usher type 1C gene. *Nat. Genet.* **26**, 56–60 (2000).
7. Verpy, E. *et al.* A defect in Harmonin, a PDZ domain-containing protein expressed in the inner ear sensory hair cells, underlies Usher syndrome type 1C. *Nat. Genet.* **26**, 51–55 (2000).
8. Kimberling, W.J. *et al.* Frequency of Usher syndrome in two pediatric populations: Implications for genetic screening of deaf and hard of hearing children. *Genet. Med.* **12**, 512–516 (2010).

9. Ouyang, X.M. *et al.* Characterization of Usher syndrome type I gene mutations in an Usher syndrome patient population. *Hum. Genet.* **116**, 292–299 (2005).
10. Ebermann, I. *et al.* Deafblindness in French Canadians from Quebec: a predominant founder mutation in the *USH1C* gene provides the first genetic link with the Acadian population. *Genome Biol.* **8**, R47 (2007).
11. Ouyang, X.M. *et al.* USH1C: a rare cause of USH1 in a non-Acadian population and a founder effect of the Acadian allele. *Clin. Genet.* **63**, 150–153 (2003).
12. Lentz, J. *et al.* The USH1C 216G→A splice-site mutation results in a 35-base-pair deletion. *Hum. Genet.* **116**, 225–227 (2005).
13. Lentz, J., Pan, F., Ng, S.S., Deininger, P. & Keats, B. Ush1c216A knock-in mouse survives Katrina. *Mutat. Res.* **616**, 139–144 (2007).
14. Lentz, J.J. *et al.* Deafness and retinal degeneration in a novel USH1C knock-in mouse model. *Dev. Neurobiol.* **70**, 253–267 (2010).
15. Hardisty-Hughes, R.E., Parker, A. & Brown, S.D. A hearing and vestibular phenotyping pipeline to identify mouse mutants with hearing impairment. *Nat. Protoc.* **5**, 177–190 (2010).
16. Michalski, N. *et al.* Harmonin-b, an actin-binding scaffold protein, is involved in the adaptation of mechanoelectrical transduction by sensory hair cells. *Pflugers Arch.* **459**, 115–130 (2009).
17. Grillet, N. *et al.* Harmonin mutations cause mechanotransduction defects in cochlear hair cells. *Neuron* **62**, 375–387 (2009).
18. Lefèvre, G. *et al.* A core cochlear phenotype in USH1 mouse mutants implicates fibrous links of the hair bundle in its cohesion, orientation and differential growth. *Development* **135**, 1427–1437 (2008).
19. Boëda, B. *et al.* Myosin VIIa, harmonin and cadherin 23, three Usher I gene products that cooperate to shape the sensory hair cell bundle. *EMBO J.* **21**, 6689–6699 (2002).
20. Peng, A.W., Salles, F.T., Pan, B. & Ricci, A.J. Integrating the biophysical and molecular mechanisms of auditory hair cell mechanotransduction. *Nat. Commun.* **2**, 523 (2011).
21. Müller, M., von Hunerbein, K., Hoidis, S. & Smolders, J.W. A physiological place-frequency map of the cochlea in the CBA/J mouse. *Hear. Res.* **202**, 63–73 (2005).
22. Greenwood, D.D. A cochlear frequency-position function for several species—29 years later. *J. Acoust. Soc. Am.* **87**, 2592–2605 (1990).
23. Hua, Y. *et al.* Peripheral SMN restoration is essential for long-term rescue of a severe spinal muscular atrophy mouse model. *Nature* **478**, 123–126 (2011).
24. Wheeler, T.M. *et al.* Targeting nuclear RNA for *in vivo* correction of myotonic dystrophy. *Nature* **488**, 111–115 (2012).
25. El-Amraoui, A. & Petit, C. Usher I syndrome: unravelling the mechanisms that underlie the cohesion of the growing hair bundle in inner ear sensory cells. *J. Cell Sci.* **118**, 4593–4603 (2005).
26. Petit, C. & Richardson, G.P. Linking genes underlying deafness to hair-bundle development and function. *Nat. Neurosci.* **12**, 703–710 (2009).
27. Hall, J.W. III. Development of the ear and hearing. *J. Perinatol.* **20**, S12–S20 (2000).
28. Uhlmann, R.A., Taylor, M., Meyer, N.L. & Mari, G. Fetal transfusion: the spectrum of clinical research in the past year. *Curr. Opin. Obstet. Gynecol.* **22**, 155–158 (2010).

ONLINE METHODS

Oligonucleotide synthesis. The synthesis and purification of all 2′O–methoxyethyl–modified oligonucleotides with phosphorothioate backbone and all 5–methyl cytosines, was performed as described[29]. The oligonucleotides were dissolved in 0.9% saline and stored at –20 °C. Sequences are shown in **Supplementary Table 1**.

Plasmids. The minigene expression plasmids pCI–Ush1C_216G and pCI–Ush1C_216A were constructed by amplifying genomic DNA from lymphoblast cell lines derived from an individual with Usher syndrome homozygous for the *USH1C* c.216G>A mutation *USH1C.216AA* (GM09458, Coriell Institute) or a healthy individual (GM09456, Coriell Institute). PCR primers specific for the 5′ end of exon 2 with restriction sites for XhoI and for the 3′ end of exon 4 with a restriction site for NotI at the 3′ end were used to amplify by PCR the *USH1C* 216A minigene fragment. The PCR product was purified and digested with XhoI and NotI and ligated into the expression plasmid pCI expression vector (Promega) digested with the same restriction enzymes.

Cell culture. Plasmids (1 μg) expressing a minigene of human *USH1C 216A* exons 2–4 and ASOs (50 nM final concentration) were transfected into HeLa cells using Lipofectamine 2000 (Life Technologies). Forty-eight hours after transfection, RNA was isolated using Trizol reagent (Life Technologies) and analyzed by radioactive RT-PCR with the primers pCI FwdB and pCI Rev **(Supplementary Table 1)** to plasmid sequences flanking exon 2 and exon 4.

Mice. *Ush1c* 216A knock-in mice were obtained from LSUHSC[13] and bred and treated at Rosalind Franklin University of Medicine and Science (RFUMS). All procedures met the NIH guidelines for the care and use of laboratory animals and were approved by the Institutional Animal Care and Use Committees at RFUMS and LSUHSC. Mice were genotyped using ear punch tissue and PCR as described previously[14]. For all studies, both male and female mice were used in approximately equal proportions. For studies in adult mice (**Fig. 1e**,**f**), homozygous 216AA mice (2–4 months of age) were injected intraperitoneally with the indicated ASO at indicated dose twice a week for 2 weeks (4 doses). RNA was isolated from different tissues 24 hrs after final injection using Trizol reagent (Life Technologies) and analyzed by radioactive RT-PCR using primers musUSH1Cex2F and musUSH1Cex5F **(Supplementary Table 1)** of the *Ush1c* 216A transgene. Products were separated on a 6% nondenaturing polyacrylamide gel and quantified using a Typhoon 9400 phosphorimager (GE Healthcare). For studies in neonate mice, pups were injected with 300 mg per kg body weight of 2′MOE ASOs at different ages, post-natal day 3–16 (P3–P16), as indicated, by intraperitoneal injection. After ABR analysis, mice were killed and tissues were collected. For ABR analysis, mice were shipped to LSUHSC 2–3 weeks after treatment. ABR was carried out at least 3 d after mice arrived.

Splicing and protein analysis. Retinae and inner ears were isolated, and cochleae and vestibules were separated and immediately frozen in liquid nitrogen or stored in Trizol reagent. For immunoblot analysis, proteins were obtained from homogenization in a modified RIPA buffer[30] or isolated from Trizol reagent (Life Technologies) according to the manufacturer's instructions. Proteins were separated on 4–15% Tris-glycine gradient gels, transferred to membrane and probed with USH1C- (20900002, Novus Biologicals) or β-actin– (Sigma-Aldrich) specific antibodies. Blots were quantified using ImageJ v1.45s software (NIH). RNA was isolated from different tissues using Trizol reagent (Life Technologies) and analyzed by radioactive RT-PCR using primers musUSH1Cex2F and musUSH1Cex5F of the *Ush1c* 216A transgene. Briefly, 0.25–1 μg of RNA was reverse transcribed using GoScript Reverse Transcriptase (Promega, Fitchburg, WI), and 1 μl of cDNA was used in PCR reactions with GoTaq Green (Promega) supplemented with primers and 0.1–.25 μl of α-32P-dCTP. Products were separated on a 6% nondenaturing polyacrylamide gel and quantified using a Typhoon 9400 phosphorimager (GE Healthcare).

Behavioral analysis. Behavioral tests were performed according to previously established protocols[15]. Investigators were blinded except in cases where the phenotype made the treatment/genotype status obvious. To quantify circling behavior, mice were placed in an open-field chamber, and behavior was analyzed using ANY-maze behavioral tracking software (Stoelting Co). Ear-twitch, startle and freezing behavior in response to a high-amplitude sound was measured by observing mouse activity following a short whistle (**Supplementary Fig. 4**). Swim tests were performed by placing mice in a tub of room-temperature water and observing their swimming behavior for 10 s. Contact-righting reflex testing was performed by placing the mouse into a closed clear tube or box and measuring the time it took to right when turned upside down. The trunk-curl test was performed by holding the tail and observing whether the mouse reached for a nearby surface or curled toward the base of its tail.

Auditory-evoked brain stem response. Hearing thresholds of treated and untreated *Ush1c* 216GG, 216GA and 216AA mice were measured by auditory-evoked brain stem response (ABR). Mice were anesthetized (intraperitoneal ketamine, 100 mg per kg body weight; xylazine, 6 mg per kg body weight), and body temperature was maintained near 38 °C with a heat pad. All recordings were conducted in a sound-proof room. Stimuli consisted of 5-ms pulses of broad-band noise, 8, 16 and 32 kHz, with 0.5-ms linear ramps. Although these tone stimuli encompass low, medium and high regions of mouse spectral sensitivity, BBN was included to confirm that responses are representative of the whole cochlear response. The stimuli were broadcast through a Motorola piezoelectric speaker (model no. 15D87141E02) fitted with a plastic funnel and 2-mm-diameter tubing over the speaker front, producing an acoustic wave guide which was positioned in the external meatus approximately 0.5 cm from the tympanum. Using continuous tones, stimulus amplitude was calibrated at the end of the tubing with a Bruel and Kjaer 2610 measuring amplifier (fast, linear weighting), 4135 microphone (grid on) and 4230 pistonphone calibrator. All stimulus amplitudes were dB SPL (re. 20 μPa). Total harmonic distortion was –40 dB (Hewlet Packard 3562A Signal Analyzer). Stimuli were generated (195 kHz srate) and responses digitized (10 kHz srate) using TDT System III hardware and software (BioSig). ABRs were recorded with a 30-gauge subdermal steel electrode placed subcutaneously behind the left ear, with indifferent and ground electrodes (steel wire, 30-gauge) placed subcutaneously at the vertex and hind limbs, respectively. After amplification (60 dB, Grass P5 AC), filtering (0.3 Hz–1 kHz; TDT PF1), and averaging (n = 600–1,024), thresholds (± 6 dB) were determined by eye as the minimum stimulus amplitude that produced an ABR wave pattern similar to that produced for the highest intensity stimulus (90 dB).

Scanning electron microscopy. The scanning electron microscopy analysis was performed as has been previously described[14]. Specifically, intralabyrinthine perfusion with fixative (2.5% glutaraldehyde/1% paraformaldehyde/1.5% sucrose in 0.12 M phosphate buffer (pH 7.4)) was performed on whole cochleae dissected from mice at P18. Cochleae were post-fixed by immersion in the same fixative for 1 d at 4 °C with gentle rotation followed by three washes in 0.12 M phosphate-buffered saline (PBS) and stored for 1 week at 4 °C. Cochleae were next fixed in 1% OsO_4 in PBS for 40 min and washed in PBS. Specimens were then serially dehydrated in ethanol, dried in a critical point drier (Autosamdri-814, Tousinis Research Corporation) and mounted on aluminum stubs. The bony capsule of the cochlea, spiral ligament, stria vascularis and Reissner's membrane were removed, and the whole organ of Corti was exposed with fine dissecting instruments. Specimens were coated in gold/palladium with a Hummer VIA sputter coater (Anatech) and viewed on a JEOL JSM 6300 F scanning electron microscope. At least three individual animals representative of each experimental paradigm were analyzed.

The cochlear place-frequency map relating distance from cochlear apex and frequency is based on a tonotopic map of mice with an average basilar membrane distance from apex to base of 5.13 mm[21]. Distances were calculated using the equation: $d = 156.5 - 82.5 \times \log(f)$; d is the normalized distance from the base (%) and f the frequency in kHz[21].

Immunofluorescence. Fluorescent labeling of microdissected preparations of the organ of Corti was used to study the hair cells of 1-month-old treated and untreated mutant and control mice as described previously[14,31]. Briefly, cochleae were isolated from the auditory bulla, and a small opening was created in the apex. The stapes was removed from the oval window, and the cochleae were gently perfused with 2% paraformaldehyde in 0.1 M phosphate buffer, pH 7.4 and post-fixed by immersion for 2 h at 4 °C with gentle rocking. Tissues were washed twice with PBS following fixation and processed for immunohistochemistry. For harmonin analysis, the tectorial membrane was removed with a fine forceps, and the stria vascularis was trimmed. Tissues were blocked for 1 h at room temperature or overnight at 4 °C (harmonin analysis) in a blocking solution consisting of 10% normal donkey serum, 0.5% bovine serum albumin, 0.1% Triton X–100 and

doi:10.1038/nm.3106

0.03% saponin in PBS to reduce nonspecific binding of primary and secondary antibodies. Primary antibody incubations were then performed at 4 °C in PBS containing 5% normal donkey serum, 0.05% bovine serum albumin, 0.1% Triton X-100 and 0.03% saponin in PBS. For counting cells, a mouse monoclonal anti-parvalbumin antibody (parv19, P3088, Sigma, 1:250) was used to label cochlear hair cells[32]. To analyze harmonin b expression, polyclonal rabbit anti-harmonin antibodies specific to isoform b (gift from U. Wolfrum, 1:100) were used. For mouse antibodies against parvalbumin, the M.O.M. kit was used as specified by the manufacturer (Vector Labs). Tissues were washed (three times for 10–15 min each) after primary and secondary antibody (donkey anti-mouse Alexa555 (A31570) and Donkey anti-rabbit Alexa488 (A21206), 1:400, Life Technologies). incubations in 0.1% Tween-20 in PBS, and nuclei were counterstained with DAPI (1 μg/ml; D9542, Sigma-Aldrich). F-actin was labeled with rhodamine phalloidin (Life Technologies) according to the manufacturer's instructions. For counting hair cells, specimens were dehydrated through an ethanol series, cleared with methyl salicylate:benzl benzoate (5:3) and examined by confocal fluorescence microscopy. For harmonin b analysis, labeled specimens were mounted and stored in Prolong Gold (Life Technologies). All samples were imaged with a Zeiss motorized system operated with LSM software (Zeiss) and equipped with 405-, 543- and 633-nm diodes along with a multiline argon laser (457 nm, 488 nm, 515 nm); an XYZ stage; and several objectives that include the Plan-NEOFLUAR 10× (NA = 0.3), Plan-NEOFLUAR 40× (NA = 1.3 oil) and Plan-APOACHROMAT 100× (NA = 1.4 oil) used. Scans were performed through a sequential (line) mode and PMT voltages dynamically regulated to compensate for signal loss due to scatter and depth limitations. Planes were captured at a resolution of 2048 × 2048 pixels and speeds of 1–2 μs per pixel. Optical volumes were deconvolved with a constrained maximum likelihood estimation algorithm and a calculated point spread function using Huygens Professional 4.1 (Scientific Volume Imaging) running on a Mac Pro computer (Apple). Z-stack images were reconstructed and analyzed using ImageJ, Fuji and Photoshop softwares.

Statistical analyses. Data were analyzed by ANOVA with *post hoc* tests and Student's *t*-test (SAS Institute Inc, NC or Prism 5 Graphpad Software) as noted in the figure legends. Hair cell counts were analyzed as the dependent variable separately for both inner and outer hair cells in a nested ANOVA with a two-level factorial arrangement of treatments[33]. The nested effect was the mice within each genotype treatment combination, the two main effect factors were cell location in the cochlea and genotype/treatment combination (combined into one variable with three levels, see **Fig. 4**). Adjustment for multiple comparisons conducted to separate interaction means was by a simulation method[34]. All data management and analysis was performed using programs and procedures in the Statistical Analysis System (SAS Institute).

29. Baker, B.F. *et al.* 2′-O-(2-methoxy)ethyl–modified anti-intercellular adhesion molecule 1 (ICAM-1) oligonucleotides selectively increase the ICAM-1 mRNA level and inhibit formation of the ICAM-1 translation initiation complex in human umbilical vein endothelial cells. *J. Biol. Chem.* **272**, 11994–12000 (1997).
30. Hastings, M.L. *et al.* Tetracyclines that promote SMN2 exon 7 splicing as therapeutics for spinal muscular atrophy. *Sci. Transl. Med.* **1**, 5ra12 (2009).
31. Hardie, N.A., MacDonald, G. & Rubel, E.W. A new method for imaging and 3D reconstruction of mammalian cochlea by fluorescent confocal microscopy. *Brain Res.* **1000**, 200–210 (2004).
32. Sage, C., Venteo, S., Jeromin, A., Roder, J. & Dechesne, C.J. Distribution of frequenin in the mouse inner ear during development, comparison with other calcium-binding proteins and synaptophysin. *Hear. Res.* **150**, 70–82 (2000).
33. Milliken, G.A. & Johnson, D.E. *Analysis of Messy Data Volume I: Designed Experiments* Ch. 30, 413–423 (Lifetime Learning Publications, Belmont, California, 1984).
34. Edwards, D. & Berry, J.J. The efficiency of simulation-based multiple comparisons. *Biometrics* **43**, 913–928 (1987).

Competing financial interests

F.R. may materially benefit financially through stock options in Isis Pharmaceuticals. M.L.H. and F.R. have patents pending with the United States Patent and Trademark Office for the ASOs and the targeting approach.